SCIENCE CHINA
Information Sciences

• RESEARCH PAPER •

January 2025, Vol. 68, Iss. 1, 112403:1–112403:7
https://doi.org/10.1007/s11432-024-4197-y

Achieving ultralow leakage current in Schottky-MIS cascode anode lateral field-effect diode based on AlGaN/GaN HEMT

Fangzhou WANG[1], Changhong GAO[2], Guojian DING[1*], Cheng YU[1,3], Zhuocheng WANG[3], Xiaohui WANG[1], Qi FENG[1], Ping YU[1], Peng ZUO[1], Wanjun CHEN[3*], Yang WANG[1*], Haiqiang JIA[1], Hong CHEN[1], Bo ZHANG[3] & Zeheng WANG[4*]

[1]*Songshan Lake Materials Laboratory, Dongguan 523808, China;*
[2]*School of Microelectronics, Southern University of Science and Technology, Shenzhen 518055, China;*
[3]*State Key Laboratory of Electronic Thin Films and Integrated Devices, University of Electronic Science and Technology of China, Chengdu 610054, China;*
[4]*Manufacturing, Commonwealth Scientific and Industrial Research Organisation, Lindfield NSW 2070, Australia*

Received 28 June 2024/Revised 26 August 2024/Accepted 17 October 2024/Published online 18 December 2024

Abstract In this paper, we design and fabricate a Schottky-metal-insulator-semiconductor (MIS) cascode anode GaN lateral field-effect diode (CA-LFED) to achieve ultralow reverse leakage current ($I_{\rm LEAK}$). The device based on AlGaN/GaN high-electron-mobility-transistor (HEMT) includes a normally-off MIS-controlled channel that is cascoded with a high barrier height Schottky contact. At reverse bias, the high electric-field is effectively prevented by the normally-off MIS-controlled channel edge. Together with the high barrier height Schottky contact, this feature significantly suppresses the $I_{\rm LEAK}$. Supported by the device fabrication, the CA-LFED with high breakdown voltage (BV) > 600 V shows an ultralow $I_{\rm LEAK}$ of 3.6×10^{-9} A/mm as well as a low forward voltage drop ($V_{\rm F}$) of 2.2 V. The performance suggests that the CA-LFED can be a promising candidate for ultralow $I_{\rm LEAK}$ and better $V_{\rm F}$-$I_{\rm LEAK}$ trade-off GaN power diode applications.

Keywords Schottky-MIS cascode anode, lateral field-effect diode (LFED), ultralow reverse leakage current ($I_{\rm LEAK}$), forward drop and reverse leakage trade-off, AlGaN/GaN HEMTs

Citation Wang F Z, Gao C H, Ding G J, et al. Achieving ultralow leakage current in Schottky-MIS cascode anode lateral field-effect diode based on AlGaN/GaN HEMT. Sci China Inf Sci, 2025, 68(1): 112403, https://doi.org/10.1007/s11432-024-4197-y

1 Introduction

Advances in power electronics technology require the development of high-efficient diode devices [1]. The GaN material has become a competitive candidate for fabricating high-power and high-frequency devices because of its wide band-gap, high electron mobility, and high critical electric-field [2–4]. The lateral diodes based on AlGaN/GaN high-electron-mobility-transistor (HEMT) can be used in the monolithic integrated power applications [5]. Many GaN lateral diodes have been proposed to realize the low reverse leakage current ($I_{\rm LEAK}$) as well as low forward voltage drop ($V_{\rm F}$) [6–9]. Conventional Schottky barrier diode (SBD) inherently has a low cost fabrication process [10]. Nevertheless, the Schottky contact directly withstands the high reverse potential and then presents high $I_{\rm LEAK}$. Moreover, the high resistivity AlGaN barrier exists between the two-dimensional-electron-gas (2DEG) and Schottky contact, which seriously degrades the $V_{\rm F}$ of the device. The principle of the lateral field-effect diode (LFED) based on AlGaN/GaN HEMT is reported to reduce the $V_{\rm F}$ [11]. In the GaN LFED, the anode consists of the electrically shorted source Ohmic contact and gate electrode of a normally-off GaN transistor, while the cathode is the Ohmic drain [12,13]. However, this low $V_{\rm F}$ architecture often results in a relatively high $I_{\rm LEAK}$ due to the contradictory relationship between the $I_{\rm LEAK}$ and $V_{\rm F}$. The GaN lateral diodes with various technologies,

* Corresponding author (email: dingguojian@sslab.org.cn, wjchen@uestc.edu.cn, wangyang@sslab.org.cn, zenwang@outlook.com)

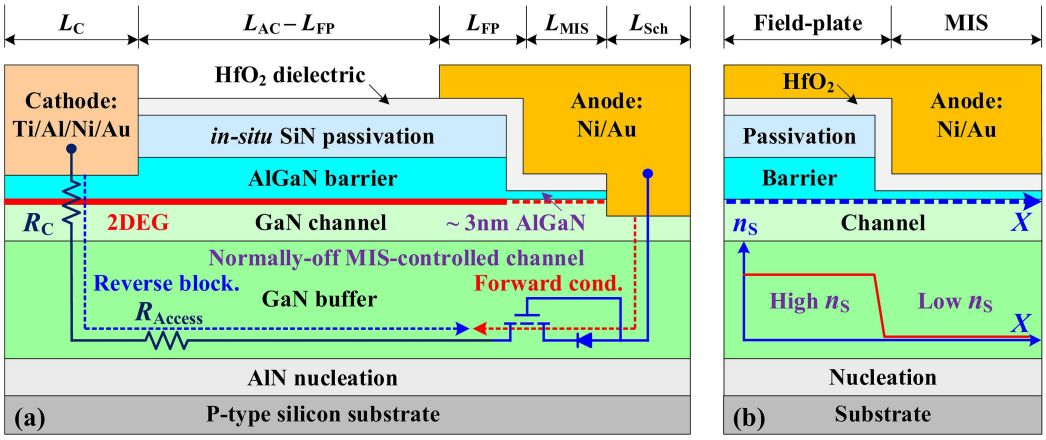

Figure 1 (Color online) Illustration of (a) device structure and (b) 2DEG density of the CA-LFED.

Table 1 Epitaxial structure and dimensional parameters.

Symbol	Quantity	Value
L_{Sch}	Schottky anode length	45 μm
L_{MIS}	MIS anode length	1.5 μm
L_{FP}	Field-plate (FP) length	2.0 μm
L_{AC}	Anode-to-cathode length	4.5/9.5/19.5 μm
L_C	Cathode length	45 μm
W	Width of the device	10 μm
t_{HfO2}	HfO_2 dielectric thickness	16 nm
t_{pass}	SiN passivation thickness	54 nm
t_{ba}	AlGaN barrier thickness	13 nm
t_{ch}	GaN channel thickness	150 nm
t_{bu}	GaN buffer thickness	4.0 μm
t_{nu}	AlN nucleation thickness	200 nm
t_{sub}	Silicon substrate thickness	800 μm
x_{ba}	AlGaN barrier Al composition	0.25

such as the recessed anode [14–16], anode field-plate (FP) [17–19], and novel epitaxial structures [20–22], are presented to suppress the I_{LEAK} and meanwhile maintain the low V_F.

In this article, we experimentally demonstrated an ultralow I_{LEAK} Schottky-MIS cascode anode LFED (CA-LFED) based on AlGaN/GaN HEMT. Cascoded at the device anode, the normally-off MIS-controlled channel and high barrier height Schottky contact prevent the high reverse electric-field and significantly suppress the I_{LEAK}. Verified by the device fabrication, the proposed CA-LFED shows an ultralow I_{LEAK} of 3.6×10^{-9} A/mm and a better V_F-I_{LEAK} trade-off.

2 Device structure and fabrication process

Figure 1 illustrates the device structure and anode 2DEG density (n_S) of the CA-LFED. To ensure good electrical properties of the fabricated devices, the in-situ SiN passivation is utilized in this work [23]. Table 1 lists the epitaxial structure and dimensional parameters of the device. The CA-LFED features the cascoded normally-off metal-insulator-semiconductor (MIS)-controlled channel and high barrier height Schottky contact. Its equivalent circuit could be considered a normally-off HEMT and an SBD with the anode-to-gate and cathode-to-source connections. The HfO_2 has a high dielectric constant (high-k). At reverse bias, the normally-off MIS-controlled channel with a Ni/HfO_2/AlGaN structure can fully deplete the 2DEG underneath. With the contribution of high barrier height Ni/GaN Schottky contact, the high reverse electric-field can be prevented to achieve an ultralow I_{LEAK} in the CA-LFED. Additionally, the 2DEG density of the normally-off MIS-controlled channel can be recovered at a low forward bias because of its relatively low threshold voltage (V_{TH}), ensuring a low V_F of the CA-LFED.

Figure 2 presents the fabrication process flow of the CA-LFED. At first, the device fabrication started

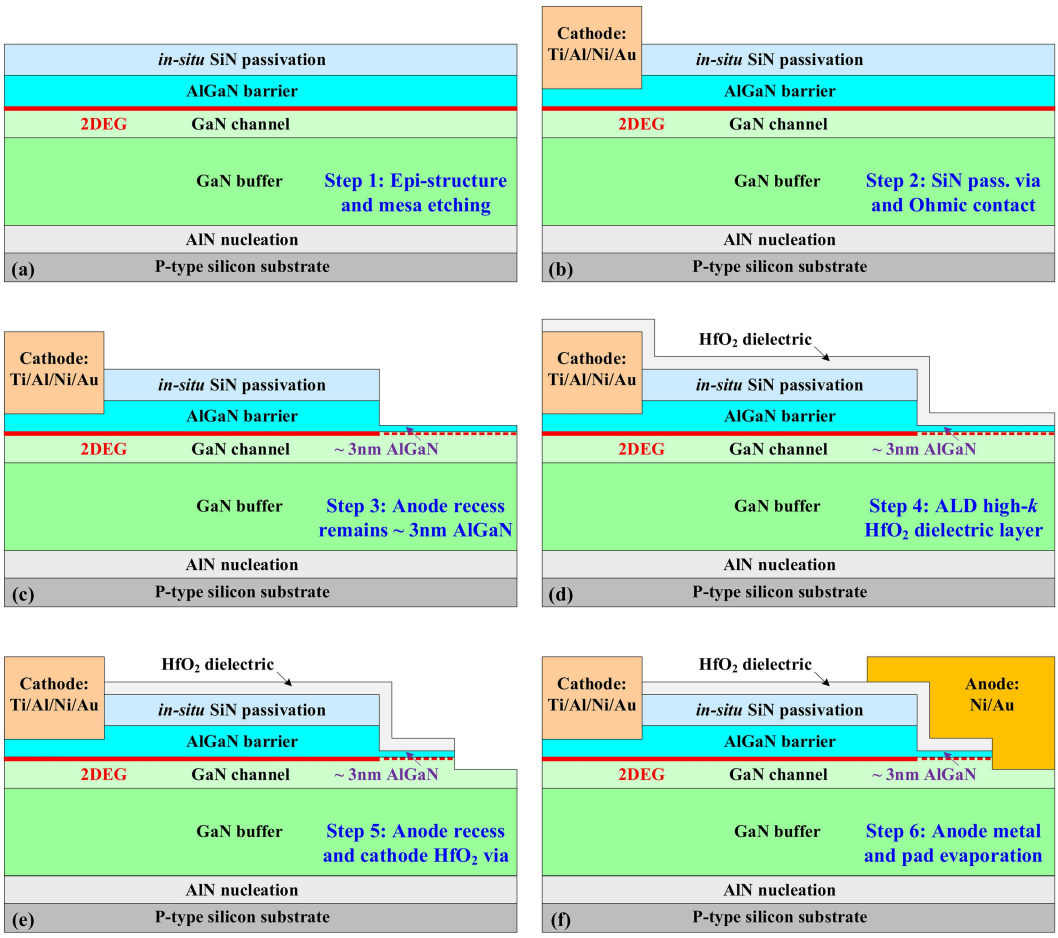

Figure 2 (Color online) Fabrication process flow of the CA-LFED. (a) Step 1: epi-structure and mesa etching; (b) step 2: passivation via and Ohmic contact; (c) step 3: anode recess remains 3 nm AlGaN; (d) step 4: ALD high-k HfO_2 dielectric layer; (e) step 5: anode recess and cathode HfO_2 via; (f) step 6: anode metal and pad evaporation.

with the epi-structure preparation and mesa etching. The SF_6/CHF_3 and the Cl_2/BCl_3 mixture gases were used to etch the in-situ SiN passivation and AlGaN/GaN hetero-structure, respectively (Figure 2(a)). The atomic force microscopy (AFM) indicated that the etching depth is about 500 nm. Then, to form the cathode Ohmic contact, the Ti/Al/Ni/Au (20/150/55/45 nm) metal stack was deposited after etching the in-situ SiN passivation (Figure 2(b)), followed by the 850°C annealing for 30 s in the N_2 ambient. The transmission-line-model (TLM) results for the sheet resistance (R_{SH}) and Ohmic contact resistance (R_C) are 580 Ω/sq and 1.5 Ω·mm, respectively. After that, for the anode recess structure of the normally-off MIS-controlled channel, the in-situ SiN passivation and the AlGaN barrier are etched with the remained AlGaN about 3 nm (Figure 2(c)). After etching the anode, the AFM morphology demonstrated in Figure 3 suggests that the etching depth is estimated to be about 64 nm. The 3 nm thickness AlGaN barrier beneath the MIS anode is challenging to control as it is a very small value. The variation in the etching process may cause the different etching depth, resulting in the carrier density variation under the MIS anode and impacting the I_{LEAK} and V_F performance of the CA-LFED. Here an ultralow power (5 W) BCl_3-based etch technique is developed to achieve an AlGaN etching rate of about 1.2 nm/min, which is adopted to accurately control the recess depth and guarantee the performance uniformity. Next, a 16 nm high-k HfO_2 dielectric was then deposited in the atomic layer deposition (ALD) system (Figure 2(d)). Subsequently, the remaining 3 nm AlGaN barrier, GaN channel, and ALD-HfO_2 in the anode are etched to form the anode recess structure of the high barrier height Schottky contact (Figure 2(e)). Finally, the evaporation of Ni/Au (50/150 nm) metal stack was carried out to serve as the anode metal and pads after removing the ALD-HfO_2 above the cathode (Figure 2(f)). Measurement suggests that V_{TH} of the recessed MIS-structure is 0.6 V. Microscopy image of the CA-LFED with L_{AC} = 4.5 μm is shown in Figure 4. The devices with L_{AC} = 9.5/19.5 μm are also realized in the same process for comparison.

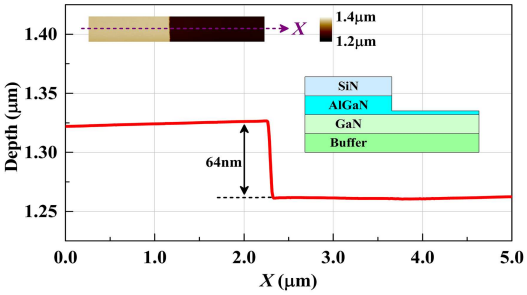

Figure 3 (Color online) AFM morphology after etching the anode in-situ SiN passivation and AlGaN barrier.

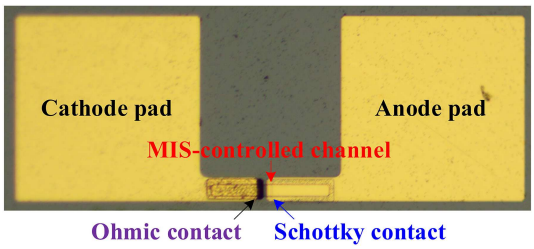

Figure 4 (Color online) Microscopy image of the fabricated CA-LFED with L_{AC} = 4.5 μm.

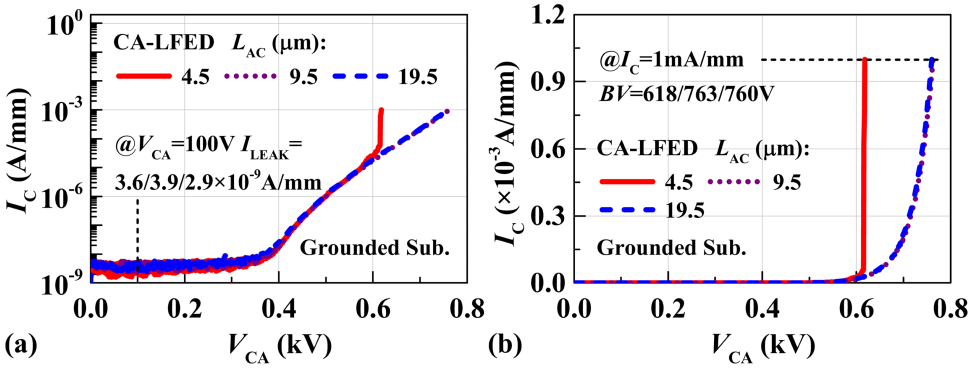

Figure 5 (Color online) (a) Log and (b) linear scale reverse I-V characteristics of the CA-LFEDs with L_{AC} = 4.5/9.5/19.5 μm.

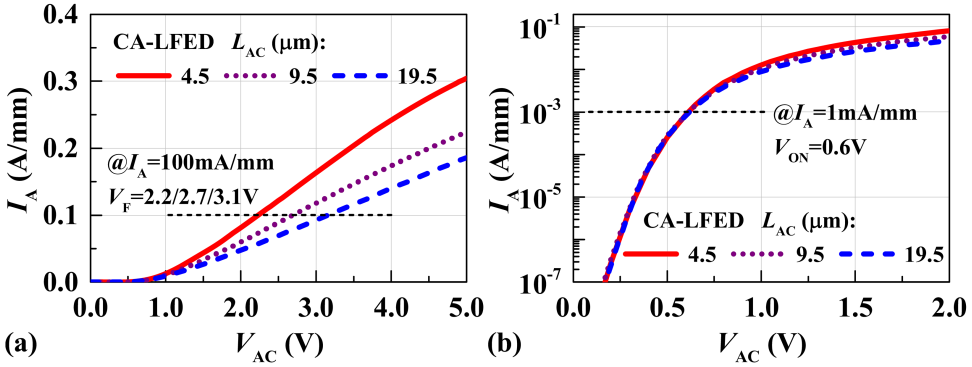

Figure 6 (Color online) (a) Linear and (b) log scale forward I-V characteristics of the CA-LFEDs with L_{AC} = 4.5/9.5/19.5 μm.

3 Results, mechanisms, and discussions

Figure 5 shows reverse I-V characteristics of the CA-LFEDs with various L_{AC}. V_{CA} and I_C are the cathode-to-anode voltage and cathode current, respectively. Both the normally-off MIS-controlled channel and high barrier height Schottky contact are beneficial to suppress the I_{LEAK}. It is suggested that the I_{LEAK} values of the CA-LFEDs maintain as low as $3.6/3.9/2.9 \times 10^{-9}$ A/mm respectively with various L_{AC} = 4.5/9.5/19.5 μm, and the devices also obtain high BVs of 618/763/760 V, respectively. Figure 6 presents forward I-V characteristics of the CA-LFEDs with various L_{AC}. The V_F and turn-on voltage (V_{ON}) are extracted at the forward current density of 100 and 1 mA/mm, respectively. V_{AC} and I_A represent the anode-to-cathode voltage and anode current, respectively. With the increase of L_{AC}, the V_F of the CA-LFED rises slightly from 2.2 to 3.1 V, while the V_{ON} is almost unchanged at 0.6 V. The forward performance indicates that the CA-LFED has an acceptable low V_F.

Figure 7 shows the lateral electric-field (E_X) and electron concentration (N_S) along the 2DEG channel in the CA-LFED. At a reverse voltage of 5 V, the electric-field peak is crowded at the normally-off MIS-

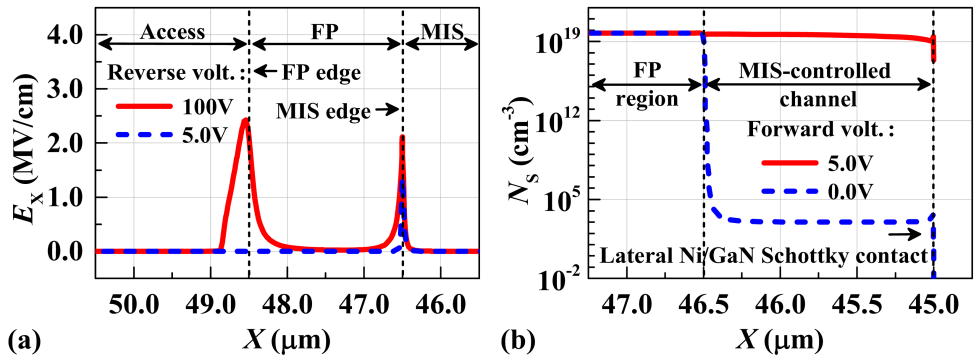

Figure 7 (Color online) (a) Lateral electric-field (E_X) and (b) electron concentration (N_S) distributions along the 2DEG channel in the CA-LFED.

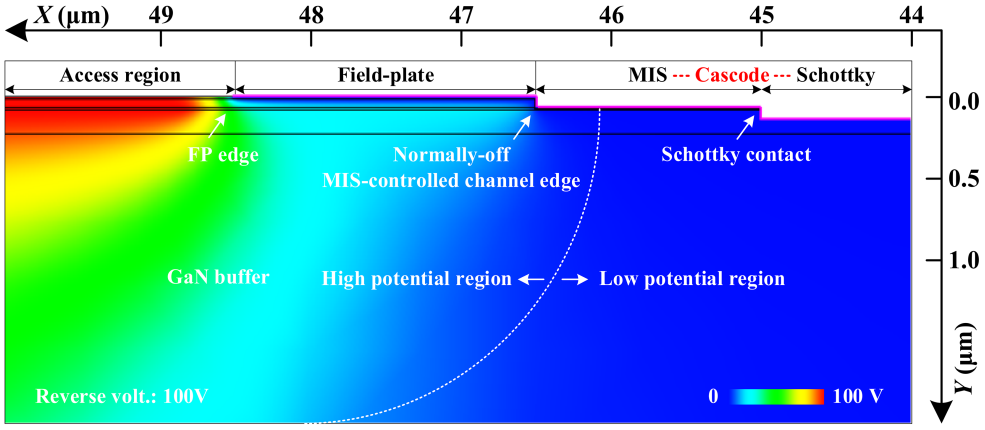

Figure 8 (Color online) Electrostatic potential distributions at a reverse voltage of 100 V in the CA-LFED.

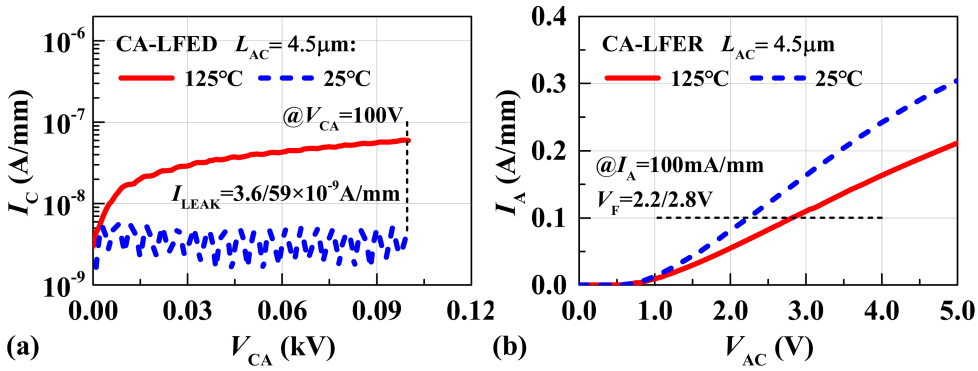

Figure 9 (Color online) High temperature (a) reverse and (b) forward I-V comparisons of the CA-LFEDs with L_{AC} = 4.5 μm.

controlled channel edge. As reverse bias increases to 100 V, the MIS edge electric-field peak is clamped. A higher electric-field peak emerges at the FP edge, suggesting that the high electric-field is effectively prevented, and the CA-LFED can present an ultralow I_{LEAK}. When forward voltage rises from 0 to 5 V, the 2DEG concentration of the normally-off MIS-controlled channel is improved to the same level as that under the FP region, indicating that the CA-LFED has a relatively low V_F. Figure 8 shows the electrostatic potential distribution at a reverse voltage of 100 V in the CA-LFED. The high potential region is located at the access region and prevented by the normally-off MIS-controlled channel and FP. This protects the Schottky contact from high reverse potential and makes the device have low I_{LEAK}. Feasibility of the simulation parameters and models has been confirmed in our previous studies [24–26].

Figure 9 shows the high temperature reverse and forward I-V comparisons of the CA-LFED with L_{AC} = 4.5 μm. The characteristics with 125°C are measured in a high temperature device test system with

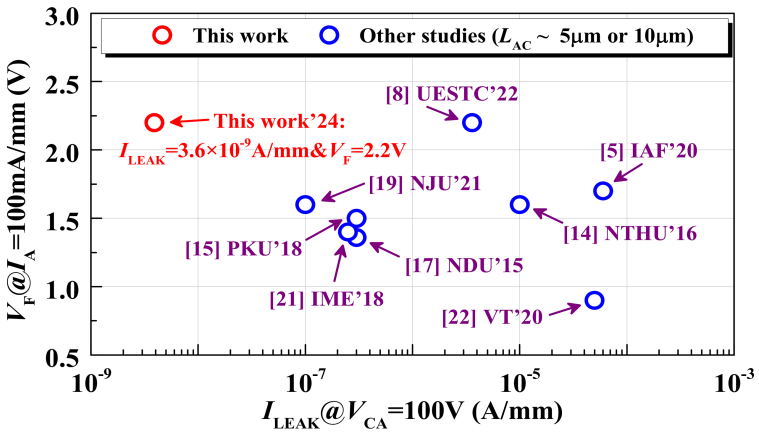

Figure 10 (Color online) V_F-I_{LEAK} comparisons of the CA-LFED and state-of-the-art devices (L_{AC} about 5 or 10 μm).

Table 2 Comparisons about the reverse leakage current and forward conduction current densities.

Ref.	Reverse leakage current (A/mm) (at V_{CA} = 100 V)	Forward conduction current (A/mm) (at V_{AC} = 3 V)
IAF'20 [5]	6.0×10^{-5}	0.20
UESTC'22 [8]	3.6×10^{-6}	0.14
NTHU'16 [14]	1.0×10^{-5}	0.17
PKU'18 [15]	2.5×10^{-7}	0.40
NDU'15 [17]	3.0×10^{-7}	0.28
NJU'21 [19]	1.0×10^{-7}	0.37
IME'18 [21]	3.0×10^{-7}	0.15
VT'20 [22]	5.0×10^{-5}	0.87
This work'24	3.6×10^{-9}	0.16

a maximum voltage of 100 V. As temperature rises from 25°C to 125°C, the I_{LEAK} in the CA-LFED increases about 16 times from 3.6×10^{-9} to 59×10^{-9} A/mm, and the V_F of the device is changed from 2.2 to 2.8 V. The V_F and I_{LEAK} at 125°C suggest that the CA-LFED exhibits excellent high temperature stability.

Figure 10 shows the V_F-I_{LEAK} comparisons of the CA-LFED and several state-of-the-art devices (L_{AC} about 5 or 10 μm). Table 2 compares this work with other lateral GaN-based diodes about the reverse leakage current and forward conduction current densities. An ultralow $I_{LEAK} = 3.6 \times 10^{-9}$ A/mm and a relatively low $V_F = 2.2$ V are obtained in the CA-LFED, verifying the ultralow leakage current of the device and suggesting the competitive V_F-I_{LEAK} trade-off among the existing studies. Additionally, compared to the standard p-GaN gate HEMT in the third quadrant [27], the CA-LFED achieves the similar I_{LEAK} as well as the lower V_F, although it has a relatively complex anode structure (pros and cons).

4 Conclusion

In this work, we propose an ultralow I_{LEAK} CA-LFED based on AlGaN/GaN HEMT. The cascoded normally-off MIS-controlled channel and high barrier height Schottky contact contribute to significantly suppressing the I_{LEAK} and meanwhile ensuring relatively low V_F. Verified by the device fabrication, the CA-LFED shows an ultralow I_{LEAK} of 3.6×10^{-9} A/mm, a relatively low V_F of 2.2 V, and a high BV > 600 V. The performance suggests that the CA-LFED can be a competitive candidate for the GaN power diode applications demanding for ultralow I_{LEAK} and a better V_F-I_{LEAK} trade-off.

Acknowledgements This work was supported in part by National Natural Science Foundation of China (Grant No. 62334003) and Guangdong Basic and Applied Basic Research Foundation (Grant No. 2020A1515110567). Zeheng WANG declares that his contribution to this research was conducted without any funding or involvement from the aforementioned funding sources.

Funding Open access funding provided by CSIRO Library Services.

References

1 Wei J, Zheng Z, Tang G, et al. GaN power integration technology and its future prospects. IEEE Trans Electron Devices, 2023, 71: 1365–1382
2 Chen K J, Haberlen O, Lidow A, et al. GaN-on-Si power technology: devices and applications. IEEE Trans Electron Devices, 2017, 64: 779–795
3 Amano H, Baines Y, Beam E, et al. The 2018 GaN power electronics roadmap. J Phys D-Appl Phys, 2018, 51: 163001
4 Buffolo M, Favero D, Marcuzzi A, et al. Review and outlook on GaN and SiC power devices: industrial state-of-the-art, applications, and perspectives. IEEE Trans Electron Devices, 2024, 71: 1344–1355
5 Basler M, Reiner R, Moench S, et al. Large-area lateral AlGaN/GaN-on-Si field-effect rectifier with low turn-on voltage. IEEE Electron Device Lett, 2020, 41: 993–996
6 Zhou Q, Liu L, Zhang A, et al. 7.6 V threshold voltage high-performance normally-off Al_2O_3/GaN MOSFET achieved by interface charge engineering. IEEE Electron Device Lett, 2015, 37: 165–168
7 Ma J, Matioli E. High-voltage and low-leakage AlGaN/GaN Tri-anode Schottky diodes with integrated tri-gate transistors. IEEE Electron Device Lett, 2016, 38: 83–86
8 Wang F, Wang Z, Chen W, et al. An ultralow turn-on gan lateral field-effect rectifier with Schottky-MIS cascode anode. IEEE Trans Electron Devices, 2022, 69: 6485–6491
9 Shao Y, Zhang F, He Y, et al. Research progress and prospect of GaN Schottky diodes. J Phys D-Appl Phys, 2023, 57: 093001
10 Lee G Y, Liu H H, Chyi J I. High-performance AlGaN/GaN Schottky diodes with an AlGaN/AlN buffer layer. IEEE Electron Device Lett, 2011, 32: 1519–1521
11 Chen W, Wong K Y, Huang W, et al. High-performance AlGaN/GaN lateral field-effect rectifiers compatible with high electron mobility transistors. Appl Phys Lett, 2008, 92: 253501
12 Chen W J, Wong K-Y, Chen K J. Single-chip boost converter using monolithically integrated AlGaN/GaN lateral field-effect rectifier and normally off HEMT. IEEE Electron Device Lett, 2009, 30: 430–432
13 Su S, Zhong Y, Zhou Y, et al. A p-GaN-gated hybrid anode lateral diode with a thicker AlGaN barrier layer. Physica Status Solidi (a), 2020, 217: 1900781
14 Tsou C W, Wei K P, Lian Y W, et al. 2.07-kV AlGaN/GaN Schottky barrier diodes on silicon with high Baliga's figure-of-merit. IEEE Electron Device Lett, 2016, 37: 70–73
15 Gao J, Jin Y, Xie B, et al. Low ON-resistance GaN Schottky barrier diode with high VON uniformity using LPCVD Si_3N_4 compatible self-terminated, low damage anode recess technology. IEEE Electron Device Lett, 2018, 39: 859–862
16 Zhang T, Zhang J, Zhou H, et al. A 1.9 kV/2.61 m$\Omega\cdot$cm^2 lateral GaN Schottky barrier diode on silicon substrate with tungsten anode and low turn-on voltage of 0.35 V. IEEE Electron Device Lett, 2018, 39: 1548–1551
17 Zhu M, Song B, Qi M, et al. 1.9-kV AlGaN/GaN lateral Schottky barrier diodes on silicon. IEEE Electron Device Lett, 2015, 36: 375–377
18 Hu J, Stoffels S, Lenci S, et al. Performance optimization of Au-free lateral AlGaN/GaN Schottky barrier diode with gated edge termination on 200-mm silicon substrate. IEEE Trans Electron Devices, 2016, 63: 997–1004
19 Xu R, Chen P, Liu M, et al. 3.4-kV AlGaN/GaN Schottky barrier diode on silicon substrate with engineered anode structure. IEEE Electron Device Lett, 2021, 42: 208–211
20 Lei J, Wei J, Tang G, et al. 650-V double-channel lateral Schottky barrier diode with dual-recess gated anode. IEEE Electron Device Lett, 2017, 39: 260–263
21 Kang X, Wang X, Huang S, et al. Recess-free AlGaN/GaN lateral Schottky barrier controlled Schottky rectifier with low turn-on voltage and high reverse blocking. In: Proceedings of IEEE 30th International Symposium on Power Semiconductor Devices and ICs (ISPSD), 2018. 280–283
22 Xiao M, Ma Y, Cheng K, et al. 3.3 kV multi-channel AlGaN/GaN Schottky barrier diodes with P-GaN termination. IEEE Electron Device Lett, 2020, 41: 1177–1180
23 Guo H, Shao P, Zeng C, et al. Improved LPCVD-SiNx/AlGaN/GaN MIS-HEMTs by using in-situ MOCVD-SiNx as an interface sacrificial layer. Appl Surf Sci, 2022, 590: 153086
24 Wang F, Chen W, Xu X, et al. Simulation study of an ultralow switching loss p-GaN gate HEMT with dynamic charge storage mechanism. IEEE Trans Electron Devices, 2021, 68: 175–183
25 Wang F, Chen W, Sun R, et al. An analytical model on the gate control capability in p-GaN Gate AlGaN/GaN high-electron-mobility transistors considering buffer acceptor traps. J Phys D-Appl Phys, 2021, 54: 095107
26 Wang F, Chen W, Wang Y, et al. Analytically modeling the effect of buffer charge on the 2DEG density in AlGaN/GaN HEMT. IEEE Trans Electron Devices, 2023, 71: 1654–1661
27 Zhang L, Wei J, Zheng Z, et al. 700-V p-GaN Gate HEMT with low-voltage third quadrant operation using area-efficient built-in diode. In: Proceedings of IEEE 32nd International Symposium on Power Semiconductor Devices and ICs (ISPSD), 2020. 521–524